RSC Advances

REVIEW

View Article Online
View Journal | View Issue

Cite this: *RSC Adv.*, 2023, **13**, 6304

Matrix metalloproteinase profiling and their roles in disease†

Mayland Chang

Matrix metalloproteinases (MMPs) play roles in remodelling of the extracellular matrix that occurs during morphogenesis, repair, and angiogenesis. Dysregulation of extracellular matrix remodelling can lead to cell proliferation, invasion, and tissue fibrosis. Identification of a specific MMP(s) in a disease has been challenging due to the presence of 24 closely-related human MMPs, each existing in three forms, of which only one is active and capable of catalysis. This review focuses on methods for MMP profiling, with particular emphasis on the batimastat affinity resin that binds only to the active forms of MMPs and related ADAMs (a disintegrin and metalloproteinases), which are then identified by mass spectrometry. Use of the batimastat affinity resin has identified targets for intervention in several human diseases.

Received 4th November 2022
Accepted 24th January 2023

DOI: 10.1039/d2ra07005g

rsc.li/rsc-advances

1. Introduction

Matrix metalloproteinases (MMPs) are a family of enzymes whose function is to degrade components of the extracellular matrix (collagen, elastin, fibronectin, laminin, proteoglycans).[1] The extracellular matrix undergoes remodelling during processes such as morphogenesis, bone remodelling, wound repair, and angiogenesis. Conversely, dysregulated extracellular matrix remodelling can lead to cell proliferation and invasion in cancer, as well as tissue fibrosis. There are 24 human MMPs, which are summarized in Table 1. MMP-4, MMP-5, and MMP-6 not included in Table 1, as they were shown to be identical to other MMPs, and MMP-22 is a chicken MMP. MMPs are classified as collagenases (MMP-1, MMP-8, MMP-13, and MMP-18), gelatinases (MMP-2 and MMP-9), stromelysins (MMP-3, MMP-10, MMP-11, and MMP-19), matrilysins (MMP-7 and MMP-26), membrane-type (MT)-MMPs (MMP-14, MMP-15, MMP-16, MMP-17, MMP-24, and MMP-25), and others.

MMPs have similar structures, consisting of a propeptide domain, a catalytic domain containing a zinc ion, and a hemopexin domain (Fig. 1). The hemopexin domain is absent in the matrilysins and MMP-23.

MMPs are made as inactive zymogens or proMMPs (Fig. 2). Removal of the propeptide domain activates the proMMPs to their active forms. Regulation of MMPs is controlled mainly by tissue inhibitors of metalloproteinases (TIMPs). The TIMP-complexed MMPs are inactive forms of MMPs. Only the active forms of MMPs, and not the proMMPs or TIMP-MMP complexes are capable of catalysis. Thus, only the active MMPs can play roles in physiology or disease pathology. The challenge is identifying which active MMP(s) is involved in a specific disease. Most methods do not distinguish among the three forms of MMPs. One of the most widely used methods is gene expression profiling by measuring mRNA levels of MMPs. However, changes in mRNA levels do not necessarily correlate with protein abundance.[2] This article focuses on methods for MMP profiling at the protein level.

Department of Chemistry and Biochemistry, University of Notre Dame, Notre Dame, IN 46556, USA. E-mail: mchang@nd.edu

† This paper is dedicated to Professor David Lynn on the occasion of his 70th birthday.

Mayland Chang is Research Professor at the University of Notre Dame. She received her PhD degree from the University of Chicago, with David Lynn as her mentor. Subsequently, she was an NIH Postdoctoral Fellow at Columbia University with Koji Nakanishi. She worked in the industry as Senior Chemist at Dow Chemical Company, Senior Scientist IV in Drug Metabolism and Pharmacokinetics at Pharmacia Corp., and was Chief Operation Officer of University Research Network Inc., where she managed clinical trials for Wayne State University. Her research interests are in translational medicinal chemistry, understanding of human disease and design of therapeutic interventions.

2. Methods for MMP profiling

2.1. Western blot

In western blot, proteins are separated by gel electrophoresis, which are then incubated with MMP antibodies. Antibodies bound to the MMP of interest are visible, with the thickness of

Table 1 MMPs, their substrates, and role in disease

MMP	Name	Production	Substrate(s)	Role in disease	Other	References
MMP-1	Interstitial collagenase, collagenase 1	Secreted: fibroblasts, keratinocytes, endothelial cells, macrophages, hepatocytes	Collagen I, II, III, VII, VIII, X, gelatin	Arthritis, idiopathic pulmonary fibrosis, cancer	Activates proMMP-2 and proMMP-9	7
MMP-2	Gelatinase-A	Secreted: fibroblasts, keratinocytes, endothelial cells, chondrocytes, osteoblasts, leukocytes, platelets, monocytes	Gelatin, collagen I, II, III, IV, VII, X	Cancer	Activates proMMP-9 and proMMP-13	8 and 9
MMP-3	Stromelysin 1	Secreted: fibroblasts, platelets	Collagen II, IV, V, IX, X, XI, gelatin	Alzheimer's disease, Parkinson's disease	Activates proMMP1 and proMMP-13	10 and 11
MMP-7	Matrilysin	Secreted: epithelial cells, liver, pancreas, prostate, skin	Fibronectin, laminin, collagen IV, gelatin	Idiopathic pulmonary fibrosis	Activates osteopontin	12
MMP-8	Neutrophil collagenase, collagenase 2	Secreted: chondrocytes, endothelial cells, macrophages, smooth muscle cells	Collagen I, II, III, VII, VIII, X, aggrecan, gelatin	Beneficial: wound healing		13 and 14
MMP-9	Gelatinase-B	Secreted: neutrophils, macrophages, osteoblasts, epithelial cells, fibroblasts, dendritic cells, keratinocytes	Gelatin, collagen IV, V	Detrimental: diabetic foot ulcers, cerebral ischemia, traumatic brain injury		13–17
MMP-10	Stromelysin-2	Secreted: keratinocytes, macrophages, epithelium	Collagen IV, laminin, fibronectin, elastin	Head and neck cancer	Activates proMMP-1	18 and 19
MMP-11	Stromelysin-3	Secreted: fibroblasts, uterus, placenta, mammary glands	Does not cleave ECM proteins	Cancer	Activated by furin	20 and 21
MMP-12	Macrophage elastase	Secreted: chondrocytes, macrophages, osteoblasts, placenta	Elastin, fibronectin, collagen IV	COPD, pulmonary emphysema	Activates protease-activated receptor-1	22–24
MMP-13	Collagenase 3	Secreted: epithelial cells, neuronal cells, connective tissue	Collagen I, II, III, IV, IX, X, XIV, gelatin	Beneficial: wound healing. Detrimental: osteoarthritis	Activates proMMP-2 and proMMP-9	5 and 25
MMP-14	MT1-MMP	Membrane-associated: fibroblast, platelets, osteoblasts	Gelatin, fibronectin, laminin, collagen I II, III	Detrimental: melanoma	Activates proMMP-2 proMMP-8, proMMP-9, and proMMP-13	26 and 27
MMP-15	MT2-MMP	Membrane-associated: placenta, heart, brain	Gelatin, fibronectin, laminin	Ovarian cancer	Can activate proMMP-2 and proMMP-13	28
MMP-16	MT3-MMP	Membrane-associated: cardiomyocites, lungs, placenta, kidney, ovaries, intestine, prostate, spleen heart, skeletal muscle	Gelatin, fibronectin, laminin	Proliferation, invasion, and migration of cancer cells	Can activate proMMP-2 and proMMP-9	29
MMP-17	MT4-MMP	Glycosylphosphatidylinositor-anchored membrane-associated: leukocytes, brain, colon, ovaries, testicles	Fibrinogen, fibrin	Cancer	Activates ADAMTS-4	30 and 31
MMP-18	Collagenase 4	Mammary gland, placenta, lung, pancreas, ovary, small intestine, spleen, thymus, prostate, colon, heart	Collagen, gelatin	Macrophage migration		32
MMP-19	Stromelysin- 4	Leukocytes, colon, intestine, ovary, testis, prostate, thymus, spleen, pancreas, kidney, skeletal muscle, liver, lung, placenta, brain, heart	Aggrecan	Tissue homeostasis, down-regulated during malignant transformation of colon	Can activate proMMP-9	33

Table 1 (*Contd.*)

MMP	Name	Production	Substrate(s)	Role in disease	Other	References
MMP-20	Enamelysin	Secreted: dental tissue	Aggrecan	Tooth development		34
MMP-21		Secreted: leukocytes, macrophages, fibroblasts, basal and squamous cells, ovary, kidney, lung, placenta, intestine, neuroectoderm, skin, brain	Unknown	Embryogenesis and tumor progression		35 and 36
MMP-22 (chicken)		Secreted	Casein, gelatin, collagen I			37
MMP-23	CA-MMP	Membrane-associated: ovary, testicles, prostate	Gelatin	Melanoma		38 and 39
MMP-24	MT5-MMP	Membrane-associated: brain, kidney, pancreas, lung	Gelatin, fibronectin, laminin	Tumor progression and angiogenesis	Can activate proMMP-2	40
MMP-25	MT6-MMP	Membrane-associated: leucocytes, testicles, kidney, skeletal muscle	Gelatin	Cancer	Activates proMMP-2	41
MMP-26	Matrilysin-2		Collagen IV, fibronectin, fibrinogen, gelatin, vitronectin	Cancer	Activates proMMP-9	42
MMP-27		B-lymphocytes, macrophages, endometrium, testicles, intestine, lung, skin	Gelatin	Endometrium lesions		43
MMP-28	Epilysin	Secreted: keratinocytes, epidermis, testis	Casein	Tissue homeostasis and repair		44

the protein band correlating to the amount of protein.[3] Antibodies are available for 60% of the 24 MMPs: MMP-1, -2, -3, -7, -8, -9, -10, -11, -12, -13, -14, -21, -25, -26, and -28.

2.2. Gelatin zymography

In zymography, MMP activity is visualized by substrate conversion and detection of the reaction product or disappearance of the substrate.[4] In this method, a substrate is polymerized with acrylamide in sodium dodecyl sulfate (SDS)-polyacrylamide gel electrophoresis (PAGE), separating proteins by mass. The most widely used method is gelatin zymography, which detects the gelatinases MMP-2 and MMP-9. This method discriminates proMMPs, however it does distinguish between active unregulated MMPs and TIMP-complexed MMPs because under the denaturing conditions, the TIMP-MMP non-covalent complexes dissociate and appear as active MMP bands. For example, analyses of non-diabetic mouse wounds by gelatin zymography showed the presence of proMMP-9, proMMP-2, and active MMP-2 on days 7 and 10 after wound infliction (Fig. 3A).[5] However, active MMP-2 was not observed in these wounds by the batismastat affinity resin/proteomics analysis, suggesting that the observed active MMP-2 band may be in complex with TIMP. To confirm the results, western blot analysis with TIMP-1 and TIMP-2 antibodies showed the presence of TIMP-1 and TIMP-2 in the samples (Fig. 3B and C), suggesting that the active MMP-2 band in Fig. 3A may be MMP-2-TIMP. Immunoprecipitation with TIMP-2 antibody, followed by western blot found that MMP-2 was present together with TIMP-2, indicating that indeed MMP-2 was in complex with TIMP (Fig. 3D and E). Since the TIMP-MMP-2 complex is catalytically incompetent, MMP-2 does not play a role in wound pathology or repair.

2.3. *In situ* zymography

In situ zymography detects and localizes MMP activity in tissue sections. In this method, tissue is embedded and cryosectioned, and the sections are placed on glass slides. The slides are immersed in dye quenched (DQ)-collagen for collagenase activity (MMP-1, MMP-8, MMP-13) or DQ-gelatin for gelatinase activity (MMP-2 and MMP-9), and analysed by fluorescence microscopy, where activity appears as green fluorescence. Fig. 4 shows the use of *in situ* zymography in diabetic wounds.

2.4. Activity-based profiling

Activity-based protein profiling (Fig. 5) uses protein engineering to introduce a cysteine nucleophile in the active site proximity that is irreversibly labelled by the affinity-based probe containing a reactive hydroxamate.[46] This method images and inhibits the specific MMP. This approach has been demonstrated for MMP-12 and MMP-14.[47] While this strategy targets only the active forms of MMPs, it requires protein engineering of MMPs and synthesis of activity-based probes for the specific MMP.

In a related approach, the zinc-chelating hydroxamate is coupled to a photocrosslinker that binds covalently only to the active forms of MMPs. The affinity-based probe contains a biotin group that allows for purification of the bound MMPs, which are identified by mass spectrometry.[48] Cells were incubated with a cocktail library of affinity-based probes that

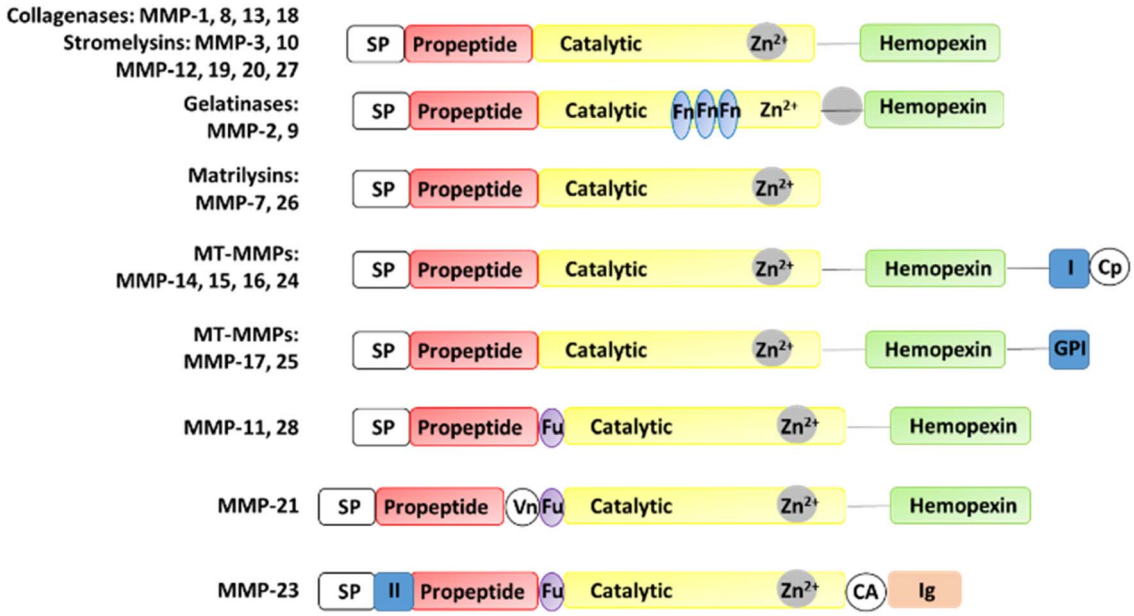

Fig. 1 Structures of MMPs. CA, cysteine array region; Cp, cytoplasmic domain; Fn, fibronectin; Fu, furin cleavage site; GPI, GPI anchor; (I) type I transmembrane domain; (II) type II transmembrane domain, Ig, IgG-like domain; SP, signal peptide; Vn, vitronectin.

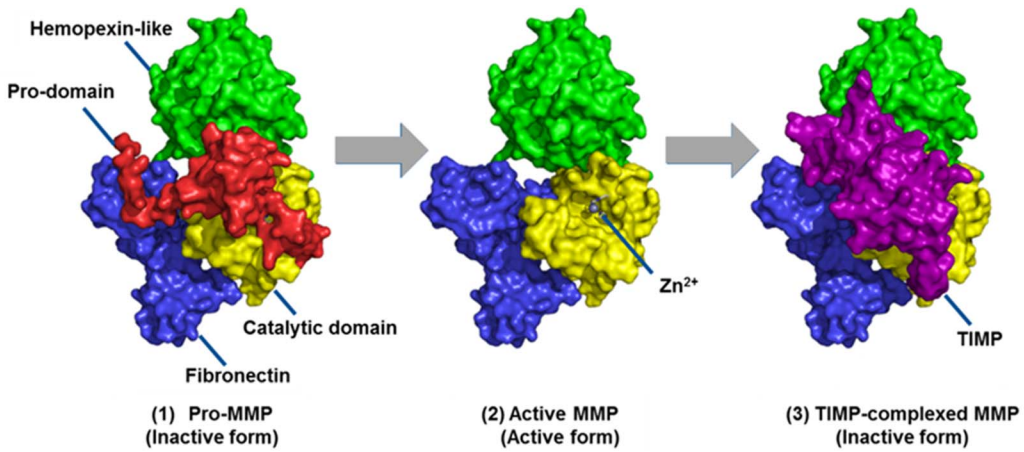

Fig. 2 The three forms of MMPs as exemplified by MMP-2. MMPs are made as inactive zymogens or proMMPs. They are activated by removal of the propeptide domain. MMPs are regulated primarily by complexation with TIMPs. This figure has been reproduced from Nguyen *et al.*[6] with permission from IntechOpen, copyright 2016.

included six MMPs.[49] This approach requires a library of selective MMP-directed probes.

2.5. Affinity resins

Affinity resins consisting of attachment of the broad-spectrum inhibitors batimastat (Fig. 6A) and TAPI-2 (Fig. 6B) inhibitors of MMPs have been covalently attached to sepharose resin.[50,51] Only the active forms of MMPs bind to the affinity resins.[52] In the case of the TAPI-2 resin, the bound MMPs are eluted with buffer containing EDTA, and following trypsin digestion the peptides are identified by mass spectrometry. TAPI-2 inhibits the related proteinases called ADAMs (a disintegrin and metalloproteinase): ADAM8 (K_i 10 ± 1 μM), ADAM10 (K_i 3 ± 2 μM), ADAM12 (K_i >100 μM), ADAM17 (K_i 120 ± 30 nM).[53] TAPI-2 also inhibits MMP-12 with a K_i value of 12 μM.[50] Given the K_i values, it appears that TAPI-2 is more selective towards ADAM17.

For the batimastat resin, cysteines in MMPs are reduced and alkylated, followed by trypsin digestion, and analysis of the resulting peptides by tandem mass spectrometry.[14,54] Batimastat is a potent broad-spectrum MMP/ADAM inhibitor with IC_{50} values of 3 nM for MMP-1,[55] 4 nM for MMP-2,[55] 20 nM for MMP-3,[55] 6 nM for MMP-7,[56] 10 nM for MMP-8,[55] 10 nM for MMP-9,[55], 1 nM for MMP-13,[56] 2.8 nM for MMP-14,[56] 29 nM for MMP-16,[57] 50 nM for ADAM8,[58] 50 nM for ADAM9,[59] and 230 nM for ADAM17.[60] The batimastat affinity resin has a limit of quantification of 6 femtomoles and recoveries for MMPs and ADAMs are similar, ranging from 75% to 100%.[61] Based on the

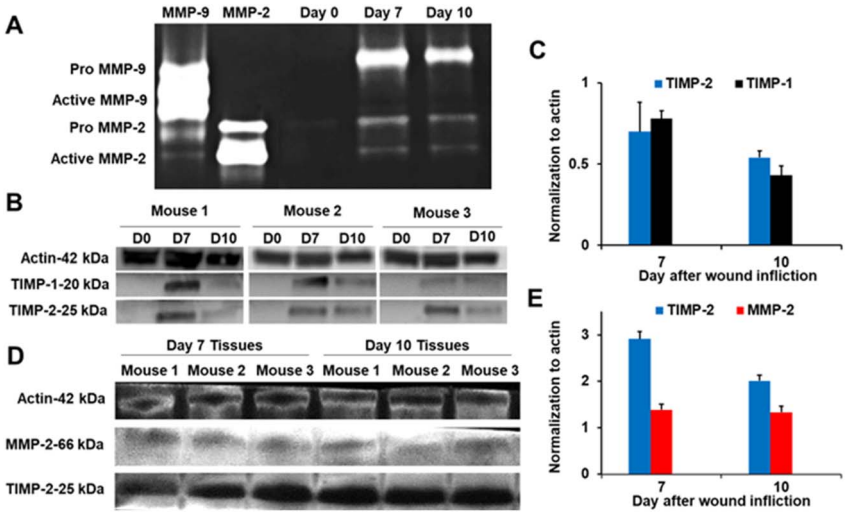

Fig. 3 (A) Gelatin zymography of non-diabetic mouse wounds shows the presence of proMMP-9, proMMP-2, and active MMP-2. (B) Analyses (n = 3 mice per time point) by western blot show the presence of TIMP-1 and TIMP-2. Actin was used as a loading control. (C) Quantification (n = 3 mice per time point) of TIMP-1 and TIMP-2 in (B). (D) Immunoprecipitation of wound homogenates (n = 3 mice per time point) with TIMP-2 antibody, followed by western-blot analysis indicates that MMP-2 is in complex with TIMP-2. (E) Quantification (n = 3 mice per time point) of TIMP-2 and MMP-2 in (D). This figure has been reproduced from Nguyen *et al.*[5] with permission from the American Chemical Society, copyright 2020.

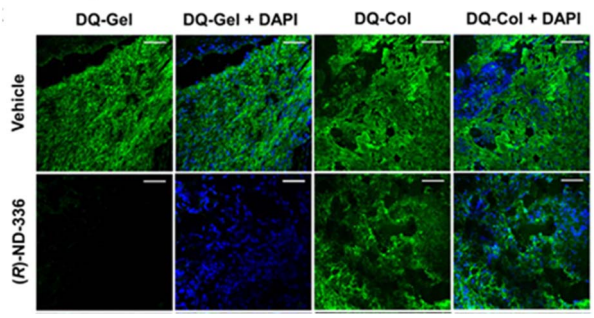

Fig. 4 Analyses of diabetic mouse wounds by *in situ* zymography with DQ-gelatin and DQ-collagen show that the MMP-9 inhibitor (*R*)-ND-336 inhibits MMP-9 activity (fluorescent green) and does not inhibit MMP-8 activity (fluorescent green). Merged images with nuclear DNA staining by DAPI (blue) as control for the number of nuclei. Images were taken with a 40× lens (scale bars, 50 μm). This figure has been reproduced from Nguyen *et al.*[45] with permission from the American Chemical Society, copyright 2018.

inhibition data, the batimastat affinity resin should be more sensitive than the TAPI-2 affinity resin. Both the TAPI-2 and batimastat affinity resins are not commercially available.

3. MMP profiling of human diseases and their roles

MMPs have been implicated in numerous diseases, including cancer, neurological diseases (Alzheimer's, Parkinson's, stroke, traumatic brain injury, spinal cord injury), pulmonary diseases such as COPD, pulmonary emphysema, idiopathic pulmonary fibrosis, and arthritis among others. Table 1 summarizes the roles of MMPs in disease.

Only the affinity-based protein profiling, the TAPI-2 affinity resin, and the batimastat affinity resin can "fish" out active MMPs, which can then be identified by mass spectrometry. An advantage of these methods is the ability to identify active MMPs in diseased tissue, rather than analyzing for specific MMPs by zymography and ELISA. The batimastat affinity resin has been used recently to identify the related proteinases ADAMs.[62,63] Bioanalytical methods have been developed to quantify the levels of active MMPs and ADAMs identified by the batimastat affinity resin.[14,54,62,63]

Once the active MMPs and ADAMs are identified in human diseased tissues and quantified relative to control tissues, the roles of the identified MMPs/ADAMs can be ascertained by use of selective inhibitors for that particular MMP/ADAM in *in vitro* or *in vivo* models of the disease. A challenge is that the 24 human MMPs and 25 human ADAMs are closely related, so selective inhibitors may not be available. Adding to the complexity is that MMPs/ADAMs can play beneficial (such as repair) and detrimental (such as pathology) roles in a disease. Confirmation of the MMP role in disease can be ascertained with MMP gene knockouts. However, gene ablation of a particular MMP may be accompanied by other effects. For example, MMP-2 knockout mice and gene ablation of MMP-8 have a compensatory increase in MMP-9.[64,65]

3.1. Diabetic foot ulcers (DFUs)

Most studies in human DFUs have used wound fluid analyzed for specific MMPs. Wound fluid from healed (n = 7) and non-healed (n = 9) DFUs were analyzed for MMP-2 and MMP-9 by zymography, and for MMP-1, MMP-8, and TIMP-1 by ELISA.[66] Active MMP-9 was not observed in the healed DFUs at inclusion, increasing to 20.85 pg μg^{-1} protein in non-healed ulcers, indicating that elevated levels of MMP-9 were detrimental to wound healing. Likewise, analysis of wound fluid from 23 healed and

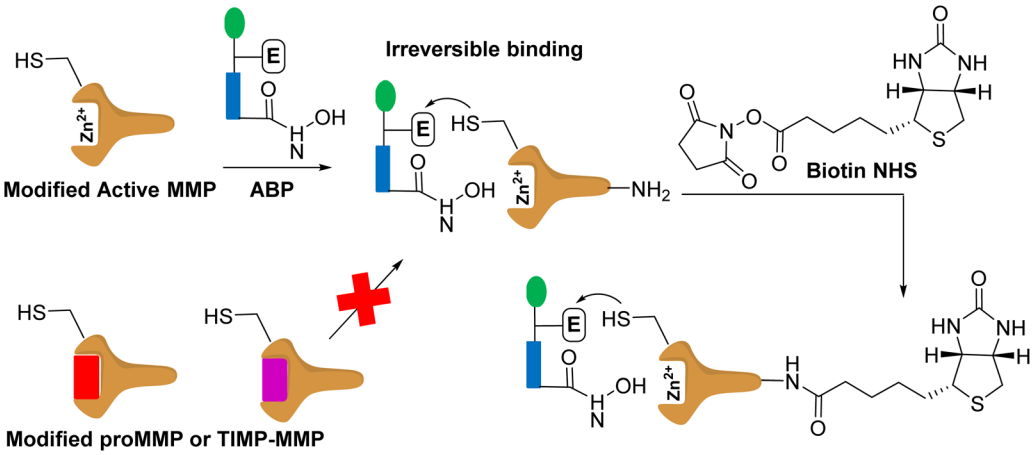

Fig. 5 Modified MMP binds to affinity based probe (APB). The modified MMP contains a cysteine. The modified active MMP binds to the ABP irreversibly. The proMMP or TIMP-MMP cannot bind to the ABP as the active site is not accessible as the prodomain and TIMP block it. The labelled active MMP can be treated with biotin for protein purification, and subsequent identification.

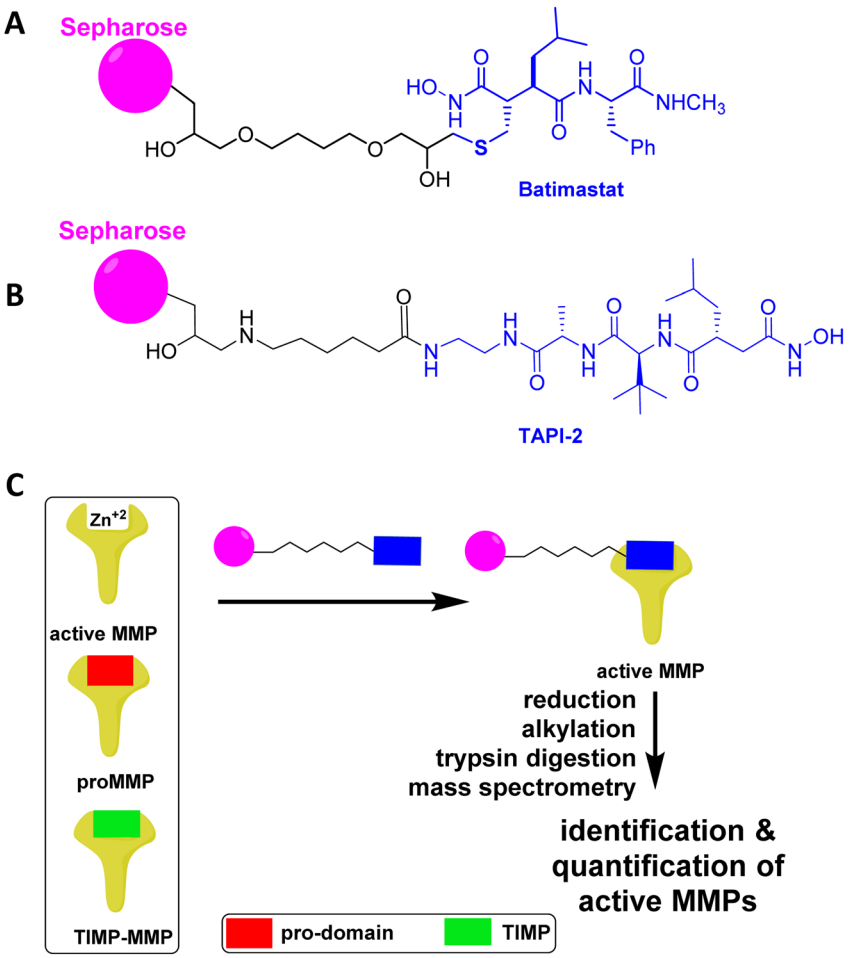

Fig. 6 Affinity resin for binding of active MMPs based on the broad-spectrum MMP inhibitor (A) batimastat or (B) TAPI-2. (C) Only the active MMPs bind to the affinity resin, as proMMPs and TIMP-MMPs do not have accessible the active site for complexation of the hydroxamate with zinc ion. (C) Analysis of the active MMPs by reduction of cysteines, alkylation of the resulting thiols, trypsin digestion, and mass spectrometry identification and quantification. Panel C is reproduced from Peng *et al.*[54] with permission from the American Chemical Society, copyright 2022.

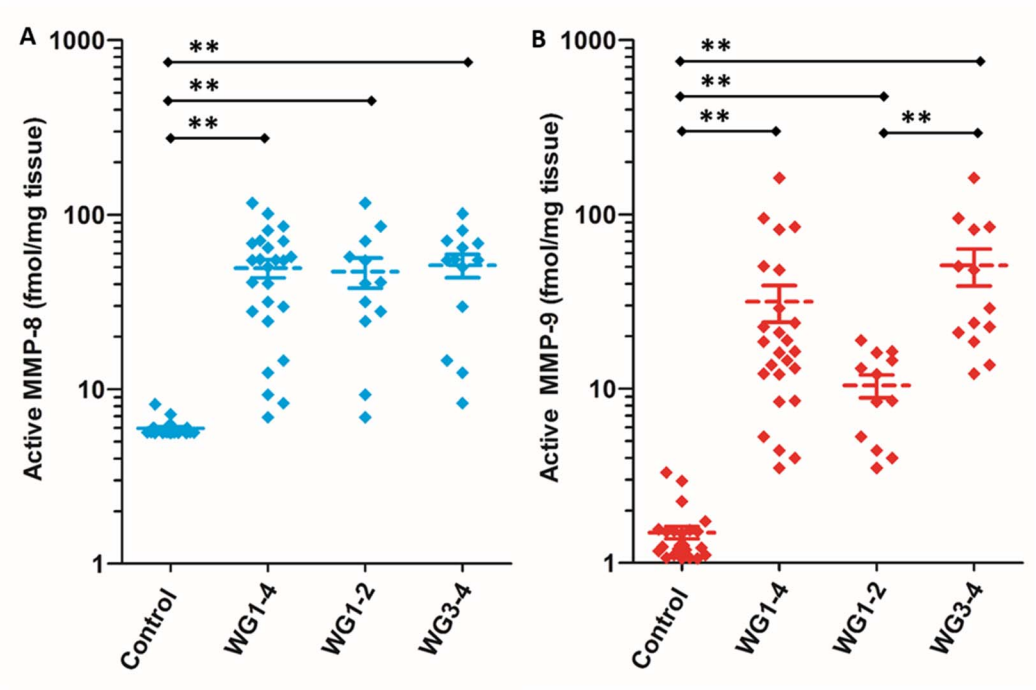

Fig. 7 Identification and quantification of (A) active MMP-8 and (B) active MMP-9 in patients with DFUs WG1–4 ($n = 25$) and in dermal samples from non-diabetic (control) patients ($n = 23$) using the batimastat affinity resin coupled with proteomics. Higher levels of active MMP-9 are observed in WG3–4 ($n = 13$) when compared to WG1–2 ($n = 12$). Mean ± SEM; $^{**}p < 0.01$ using Mann–Whitney U two-tailed test. This figure has been reproduced from Nguyen *et al.*[45] with permission from the American Chemical Society, copyright 2018.

39 non-healed DFUs by zymography found higher levels of active MMP-9 in non-healers (2.90 ± 1.64, $p < 0.05$) compared to non-healers (1.18 ± 1.21 μg mL^{-1}),[67] indicating that higher levels of MMP-9 can predict poor wound healing.

Wound tissue from patients with DFUs ($n = 25$) and non-diabetic controls ($n = 23$) were analyzed with the batimastat affinity resin. Only two MMPs in their active forms were identified: MMP-8 and MMP-9.[45] The analysis was stratified by wound

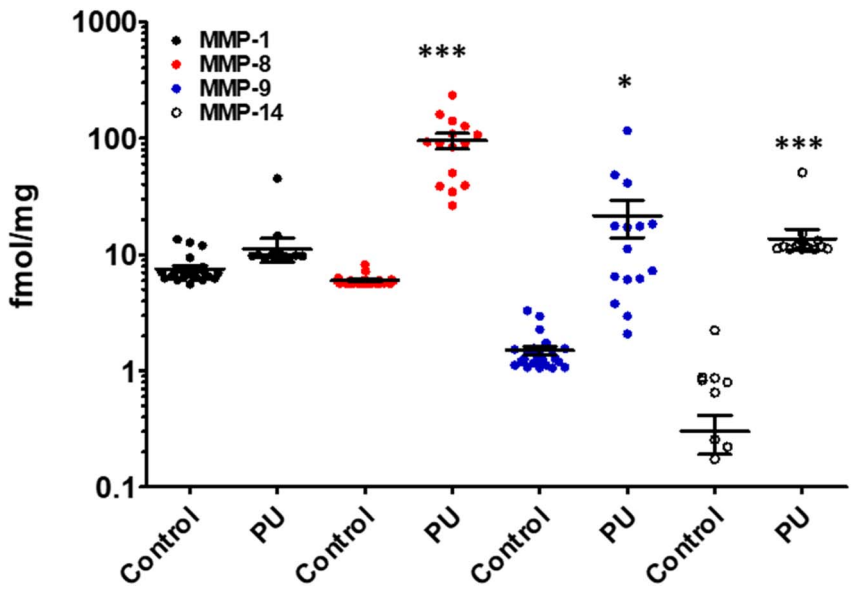

Fig. 8 Identification and quantification of active MMPs in patients with PUs using the batimastat affinity resin with proteomics. Active MMP-1, MMP-8, MMP-9, and MMP-14 were identified in wound tissue of patients at ulcer stage 3–4 PUs ($n = 15$) and in control (healthy) patients ($n = 23$). Mean ± SEM, $^{*}p < 0.05$, $^{***}p < 0.001$ by Mann–Whitney U two-tails. This figure has been reproduced from Peng *et al.*[54] with permission from the American Chemical Society, copyright 2022.

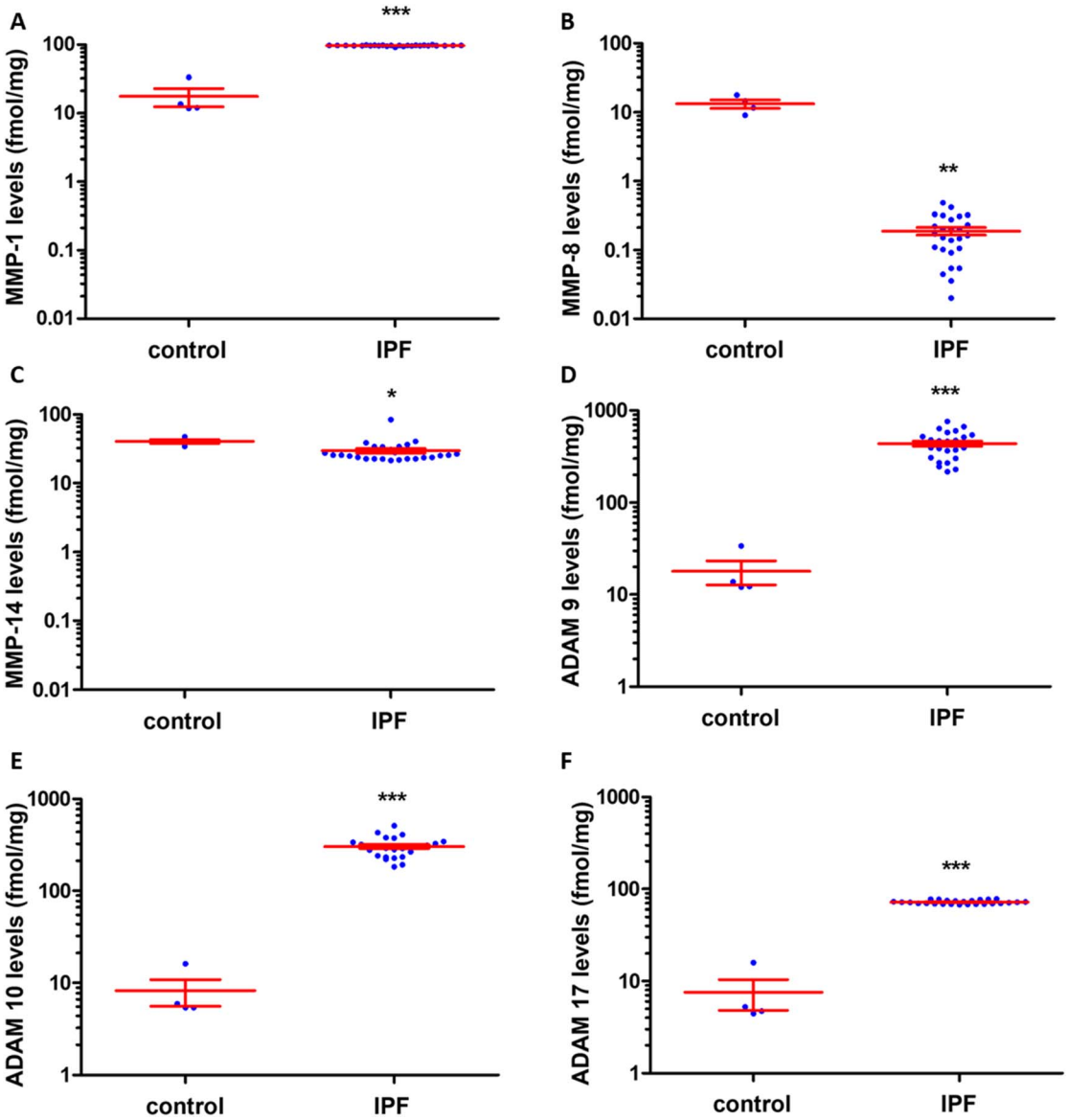

Fig. 9 Identification and quantification of active MMPs and ADAMs in lungs of patients with IPF using the batimastat affinity resin and proteomics. Higher levels of MMP-1, ADAM9, ADAM10, and ADAM17 were observed in IPF lungs. Concentrations of (A) active MMP-1, (B) active MMP-8, (C) active MMP-14, (D) active ADAM9, (E) active ADAM10, and (F) active ADAM17. IPF lung tissue ($n = 26$ patients) and healthy control lungs ($n = 4$); mean ± SEM; *$p < 0.05$, **$p < 0.01$, ***$p < 0.001$ relative to control by Student's t-test with two-tail distribution and unequal variance. This figure has been reproduced from Peng *et al.*[63] with permission from the American Chemical Society, copyright 2022.

severity and infection, with Wagner grade (WG) 1 as a superficial ulcer, 2 as a deeper full-thickness ulcer, 3 as deep abscess or osteomyelitis, and 4 as partial gangrene of the foot. MMP-8 was present at 10-fold higher levels in DFUs compared to controls; similar levels were observed regardless of wound severity and infection (Fig. 7A). In contrast, active MMP-9 concentrations increased with DFU severity and infection: 7-fold higher in WG1-2, and 34-fold higher in WG3-4 (Fig. 7B). The role of MMP-9 was found to be detrimental to wound healing using selective MMP-9 inhibitors and MMP-9 knockout mice made diabetic.[13,14] On the other hand, MMP-8 was shown to be beneficial in wound repair by the use of a selective MMP-8 inhibitor and application of exogenous recombinant MMP-8.[13,14]

3.2. Pressure ulcers (PUs)

Analysis of wound fluid from 56 patients with PUs for MMP-2, MMP-9, TIMP-1, and TIMP-2 found that the ratio of MMP-9 to TIMP-1 significantly decreased in healing PUs, supporting that high levels of MM-9 activity and low levels of TIMP-1 are detrimental to wound healing.[68]

Analyses of wound tissue from patients with PUs ulcer stage 3–4 (where stage 3 is full-thickness deep open ulcer and stage 4 is full-thickness with muscle or bone exposure) using the batimastat affinity resin and proteomics, revealed the presence of active MMP-8 and MMP-9.[54] MMP-8 was present at 16-fold higher levels in PUs relative to controls, while MMP-9 was 14-fold higher (Fig. 8).[54] The amounts of MMP-9 decreased with improvement of

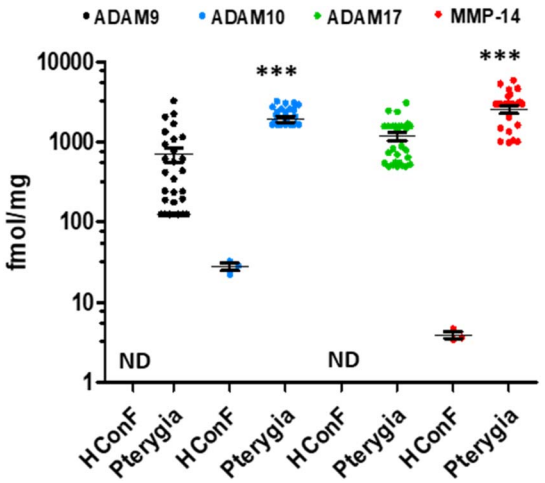

Fig. 10 Identification and quantification of active MMPs and ADAMs in pterygium tissue by the batimastat affinity resin and proteomics. Primary pterygium tissue (n = 28 patients); mean ± SEM, ND = not detectable, ***p < 0.001 by Student's t-test. This figure has been reproduced from Masitas *et al.*[62] with permission from the American Chemical Society, copyright 2022.

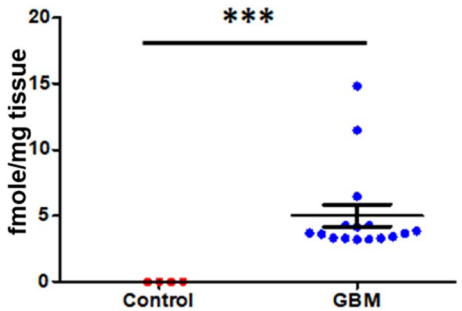

Fig. 11 Identification and quantification of active MMP-14 in brain tissue by the batimastat affinity resin and proteomics. Glioblastoma multiforme patients (n = 15), healthy controls (n = 4); mean ± SEM, **p < 0.001 by Student's t-test. This figure has been graphed from data in Thakur *et al.*[81]

PUs, indicating that MMP-9 played a detrimental role in PUs. The higher levels of MMP-8 and MMP-9 in PUs were not surprising, given that PUs share similar pathology with DFUs; in both diseases wound repair is stalled with persistent inflammation, and development of both wounds are due to neuropathy and trauma. The likelihood of developing PUs is twice as high for patients with diabetes.[69] In addition, MMP-1 and MMP-14 in their active forms were present in PUs (Fig. 8). The levels of MMP-1 in PUs were similar to those in the controls, while MMP-14 concentrations were 46-fold higher in PUs compared to the controls. Inhibition of MMP-9 and MMP-14 accelerated wound healing and improved ulcer stage in a mouse model of PUs.[54]

3.3. Idiopathic pulmonary fibrosis (IPF)

MMP-9 has been found in lungs and bronchoalveolar lavage fluid from patients with IPF.[70] MMP-9 expression increased in airway basal cells from patients with IPF relative to those from normal lungs.[71] In a mouse model of IPF, mice treated with andecaliximab, a monoclonal antibody that inhibits MMP-9, showed improved outcomes.[71,72]

Lung tissue from patients with IPF were analyzed with the batimastat affinity resin coupled with proteomics. Six proteinases MMP-1, MMP-8, MMP-14, ADAM9, ADAM10, and ADAM17 were identified.[63] Levels of MMP-1 were 1.5-fold higher in IPF compared to control (Fig. 9A), while MMP-8 levels were lower in IPF than control (Fig. 9B) and those of MMP-14 were similar in IPF and control (Fig. 9C). ADAM9 (Fig. 9D), ADAM10 (Fig. 9E), and ADAM17 (Fig. 9F) levels increased in IPF compared to controls. Inhibition of MMP-1 and ADAM10 decreased fibrosis in an *in vitro* assay,[63] indicating the potential for therapeutic intervention. Bleomycin induced lung-injured mice administered the ADAM-10 inhibitor GI254023X showed significantly reduced mortality.[73]

3.4. Pterygium

MMP-1 and MMP-3 were reported in cultured human pterygium fibroblasts by mRNA, ELISA, and western blot.[74] MMP-2 and MMP-9 were observed in pterygium tissues from 15 patients by mRNA and gelatin zymography.[75] Elevated levels of MMP-7 were reported in cultured pterygia using monoclonal antibodies.[76] MMP-1, MMP-2, and MMP-9 were found in pterygium cells by immunohistochemistry using antibodies.[77]

The batimastat affinity resin and mass spectrometry was used to identify active MMP-14, ADAM9, ADAM10, and ADAM17 in pterygium (benign ocular tumor) tissue (Fig. 10).[62] Normal human conjunctiva fibroblasts were used as control due to the unavailability of control human eye tissue for ethical reasons. Active MMP-14 and ADAM10 were about 70 times higher in patients with pterygia than controls. Inhibition of MMP-14 decreased fibroblast migration and collagen contraction in *in vitro* assays,[62] indicating a potential therapeutic approach to treat pterygium. Current treatment of pterygium is recurrent surgery.

3.5. Glioblastoma multiforme

MMP-14 (also known as membrane-type 1-matrix metalloproteinase (MT1-MMP)), has been implicated in the pathology of gliomas.[78] MMP-14 expression has been correlated to glioma cell invasiveness, with higher levels of MMP-14 expression in the most invasive U251 glioma cells compared to other cell lines.[79] In addition, MMP-14 plays a role in tumor angiogenesis through activation of MMP-2 and MMP-9.[80]

Brain tissue from patients with glioblastoma multiforme were analyzed by the batimastat affinity resin, followed by proteomics. Only MMP-14 in its active form was identified and quantified.[81] Levels of active MMP-14 were non-quatifiable in control brains and were 4.0 ± 0.8 fmol mg^{-1} tissue in brains of patients with glioblastoma multiforme (Fig. 11). Inhibition of MMP-14 with a selective inhibitor prolonged survival in mice with glioblastoma.[81]

4. MMP inhibitors in development

Recent reviews describe new strategies for targeting MMPs,[82–84] including integration of computational design and yeast surface display to engineer a TIMP-mutant that is a potent and

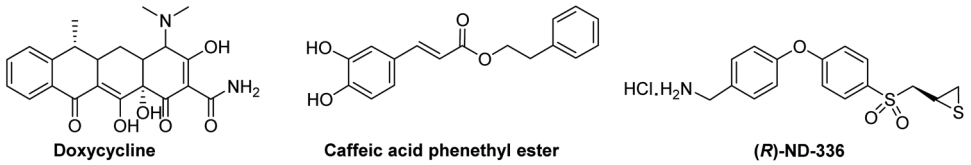

Fig. 12 Structures of MMP inhibitors.

specific inhibitor of MMP-14 (ref. 85) and MMP-responsive drug delivery and tumor targeting.[86] This section reviews MMP inhibitors in development.

The role of MMPs in promoting cancer progression prompted the development of small-molecule MMP inhibitors. At the time it was thought that all MMPs were involved in cancer progression. Thus, the initial inhibitors were broad-spectrum hydroxamate derivatives that inhibited all MMPs by chelating to zinc. Numerous MMP inhibitors were studied in clinical trials for cancer, but all failed. The reasons for failure were numerous,[87] including poor clinical trial design, broad-spectrum inhibition of MMPs and ADAMs, lack of knowledge of which MMP(s) should be targeted, undesirable side effects, poor pharmacokinetic properties, poor knowledge of MMP biology, animal models not paralleling the human disease.

To date, Periostat® (doxycycline hyclate, Fig. 12) is the only MMP-inhibitor on the market; it is approved for treatment of periodontitis. Doxycycline is a weak broad-spectrum MMP inhibitor, with IC_{50}s of >400 μM for MMP-1, 56 μM for MMP-2, 32 μM for MMP-3, 28 μM for MMP-7, 26–50 μM for MMP-8, and 2–50 μM for and MMP-13.[87]

A clinical trial was completed (NTC 02744703) in 10 patients receiving caffeic acid phenethyl ester (Fig. 12) as an MMP inhibitor for bonding of resin material and tooth substrate. Pre-treatment improved the bond strength of resin restoration to dentin. Caffeic acid phenethyl ester inhibits MMP-1 (IC_{50} 187 μM), MMP-2 (IC_{50} 5 μM), MMP-3 (IC_{50} 224 μM), MMP-7 (IC_{50} 335 μM), and MMP-9 (IC_{50} 2 μM).[88] Additional clinical trials with caffeic acid phenethyl ester have been started.[89] Two clinical trials, a phase 1 study assessing the safety and tolerability of multiple oral doses in 21 subjects with amyotrophic lateral sclerosis (NTC 03049046), and a phase 3 clinical trial in 300 patients with esophageal cancer receiving oral caffeic acid phenethyl ester (NTC 03070262) are listed in **https://clinicaltrials.gov**; no results are reported.

Andecaliximab (GS-5745) is a monoclonal antibody from Gilead Sciences, Inc. that inhibits MMP-9. In a phase 1b study, andecaliximab was evaluated alone and in combination with mFOLFOX6 (fluoracil). Encouraging results were observed in patients with gastric or gastroesophageal junction adenocarcinoma.[90] However, a phase 3 clinical trial in 432 patients with gastric or gastroesophageal junction adenocarcinoma did not improve overall survival.[91] In 2019, Gilead terminated clinical development of andecaliximab for oncology.

(*R*)-ND-336 (Fig. 12) is a thiirane mechanism-based inhibitor selective for MMP-2 (K_i 127 nM), MMP-9 (K_i 19 nM), and MMP-14 (K_i 119 nM); it inhibits other MMPs poorly ($K_{iMMP\text{-}8}$ 8590 nM, all other MMPs K_i > 100 000 nM).[45] (*R*)-ND-336 accelerates wound healing in diabetic mice,[45] including in an infected model,[92] as well as in a mouse model of pressure ulcers.[54] As MMP-9 is detrimental to diabetic wound healing, an MMP-9 siRNA hydrogel has shown efficacy in diabetic rats. Targeting MMP-14 sensitized glioblastoma to radiation; inhibition of MMP-14 with (*R*)-ND-336 significantly increased survival in a mouse model of glioblastoma multiforme[93] (survival of 77 days after irradiation compared to 148 days with combination of irradiation plus (*R*)-ND-336, $p = 0.02$).[81] (*R*)-ND-336 has completed Investigational New Drug-enabling studies.

5. Conclusions

MMP profiling is challenging due to the presence of 24 closely-related human MMPs and 25 human ADAMs, each existing in three forms, of which only one is active and capable of catalysis. This challenge has been overcome with development of affinity resins that incorporate a broad-spectrum MMP/ADAM inhibitor. In particular, the batimastat affinity resin is a potent and broad-spectrum chemical tool that captures MMPs and ADAMs in their active forms, which are subsequently identified by mass spectrometry. The batimastat affinity resin has proven useful in identifying targets for intervention in several human diseases.

Author contributions

M. C. wrote the manuscript.

Conflicts of interest

The author declares the following competing financial interests: US Patent 9,604,957, US Patent 9,951,035, US Patent 10,253,103, European Patent 3107905, Japan Patent 6,5,21,995, and China Patent ZL201580023723.6 have been issued for (*R*)-ND-336 (assigned to the University of Notre Dame, with M. C. as an inventor. M. C. reports involvement in an organization with a financial interest in (*R*)-ND-336.

Acknowledgements

M. C. was supported in part by Department of Defense Therapeutic Development Award W81XWH-19-1–0493.

Notes and references

1 H. Nagase, R. Visse and G. Murphy, *Cardiovasc. Res.*, 2006, **69**, 562–573.

2 D. Greenbaum, C. Colangelo, K. Williams and M. Gerstein, *Genome Biol.*, 2003, **4**, 117.
3 T. Mahmood and P. C. Yang, *Am. J. Med. Sci.*, 2012, **4**, 429–434.
4 J. Vandooren, N. Geurts, E. Martens, P. E. Van den Steen and G. Opdenakker, *Nat. Methods*, 2013, **10**, 211–220.
5 T. T. Nguyen, W. R. Wolter, B. Anderson, V. A. Schroeder, M. Gao, M. Gooyit, M. A. Suckow and M. Chang, *ACS Pharmacol. Transl. Sci.*, 2020, **3**, 489–495.
6 T. T. Nguyen, S. Mobashery and M. Chang, Roles of matrix metalloproteinases in cutaneous wound healing, in *Wound Healing: New Insights into Ancient Challenges*, ed. V. A. Alexandrescu, InTech, 2016, pp. 37–71.
7 A. Pardo and M. Selman, *Int. J. Biochem. Cell Biol.*, 2005, **37**, 283–288.
8 G. Klein, E. Vellenga, M. W. Fraaije, W. A. Kamps and E. S. de Bont, *Crit. Rev. Oncol./Hematol.*, 2004, **50**, 87–100.
9 R. Fridman, M. Toth, D. Pena and S. Mobashery, *Cancer Res.*, 1995, **55**, 2548–2555.
10 Y. C. Chung, Y. S. Kim, E. Bok, T. Y. Yune, S. Maeng and B. K. Jin, *Mediators Inflammation*, 2013, **2013**, 370526.
11 Y. Yoshiyama, M. Asahina and T. Hattori, *Acta Neuropathol.*, 2000, **99**, 91–95.
12 A. Pardo, K. Gibson, J. Cisneros, T. J. Richards, Y. Yang, C. Becerril, S. Yousem, I. Herrera, V. Ruiz, M. Selman and N. Kaminski, *PLoS Med.*, 2005, **2**, e251.
13 M. Gao, T. T. Nguyen, M. A. Suckow, W. R. Wolter, M. Gooyit, S. Mobashery and M. Chang, *Proc. Natl. Acad. Sci. U. S. A.*, 2015, **112**, 15226–15231.
14 M. Gooyit, Z. Peng, W. R. Wolter, H. Pi, D. Ding, D. Hesek, M. Lee, B. Boggess, M. M. Champion, M. A. Suckow, S. Mobashery and M. Chang, *ACS Chem. Biol.*, 2014, **9**, 105–110.
15 Z. Gu, J. Cui, S. Brown, R. Fridman, S. Mobashery, A. Y. Strongin and S. A. Lipton, *J. Neurosci.*, 2005, **25**, 6401–6408.
16 O. Hadass, B. N. Tomlinson, M. Gooyit, S. Chen, J. J. Purdy, C. R. I. Robinson, D. S. Shin, V. A. Schroeder, M. A. Suckow, A. Simonyi, G. Y. Sun, S. Mobashery, J. Cui, M. Chang and Z. Gu, *PLoS One*, 2013, **8**, e76904.
17 P. E. Van den Steen, B. Dubois, I. Nelissen, P. M. Rudd, R. A. Dwek and G. Opdenakker, *Crit. Rev. Biochem. Mol. Biol.*, 2002, **37**, 375–536.
18 W. B. Saunders, K. J. Bayless and G. E. Davis, *J. Cell Sci.*, 2005, **118**, 2325–2340.
19 E. M. Deraz, Y. Kudo, M. Yoshida, M. Obayashi, T. Tsunematsu, H. Tani, S. B. Siriwardena, M. R. Keikhaee, G. Qi, S. Iizuka, I. Ogawa, G. Campisi, L. Lo Muzio, Y. Abiko, A. Kikuchi and T. Takata, *PLoS One*, 2011, **6**, e25438.
20 X. Zhang, S. Huang, J. Guo, L. Zhou, L. You, T. Zhang and Y. Zhao, *Int. J. Oncol.*, 2016, **48**, 1783–1793.
21 W. Pan, M. Arnone, M. Kendall, R. H. Grafstrom, S. P. Seitz, Z. R. Wasserman and C. F. Albright, *J. Biol. Chem.*, 2003, **278**, 27820–27827.
22 I. K. Demedts, A. Morel-Montero, S. Lebecque, Y. Pacheco, D. Cataldo, G. F. Joos, R. A. Pauwels and G. G. Brusselle, *Thorax*, 2006, **61**, 196–201.
23 S. Molet, C. Belleguic, H. Lena, N. Germain, C. P. Bertrand, S. D. Shapiro, J. M. Planquois, P. Delaval and V. Lagente, *Inflammation Res.*, 2005, **54**, 31–36.
24 H. H. Hou, H. C. Wang, S. L. Cheng, Y. F. Chen, K. Z. Lu and C. J. Yu, *Am. J. Physiol.: Lung Cell. Mol. Physiol.*, 2018, **315**, L432–L442.
25 G. Tardif, P. Reboul, J. P. Pelletier and J. Martel-Pelletier, *Mod. Rheumatol.*, 2004, **14**, 197–204.
26 M. Toth, I. Chvyrkova, M. M. Bernardo, S. Hernandez-Barrantes and R. Fridman, *Biochem. Biophys. Res. Commun.*, 2003, **308**, 386–395.
27 C. Marusak, I. Bayles, J. Ma, M. Gooyit, M. Gao, M. Chang and B. Bedogni, *Pharmacol. Res.*, 2016, **113**, 515–520.
28 A. Lin, H. H. Xu, D. P. Xu, X. Zhang, Q. Wang and W. H. Yan, *Hum. Immunol.*, 2013, **74**, 439–446.
29 H. Wang, C. Qi and D. Wan, *Ann. Transl. Med.*, 2021, **9**, 124.
30 Y. Itoh, M. Kajita, H. Kinoh, H. Mori, A. Okada and M. Seiki, *J. Biol. Chem.*, 1999, **274**, 34260–34266.
31 C. Yip, P. Foidart, A. Noel and N. E. Sounni, *Int. J. Mol. Sci.*, 2019, **20**, 354.
32 J. Cossins, T. J. Dudgeon, G. Catlin, A. J. Gearing and J. M. Clements, *Biochem. Biophys. Res. Commun.*, 1996, **228**, 494–498.
33 V. O. Bister, M. T. Salmela, M. L. Karjalainen-Lindsberg, J. Uria, J. Lohi, P. Puolakkainen, C. Lopez-Otin and U. Saarialho-Kere, *Dig. Dis. Sci.*, 2004, **49**, 653–661.
34 Y. Lu, P. Papagerakis, Y. Yamakoshi, J. C. Hu, J. D. Bartlett and J. P. Simmer, *Biol. Chem.*, 2008, **389**, 695–700.
35 Y. Pu, L. Wang, H. Wu, Z. Feng, Y. Wang and C. Guo, *Oncol. Rep.*, 2014, **31**, 2644–2650.
36 G. N. Marchenko, N. D. Marchenko and A. Y. Strongin, *Biochem. J.*, 2003, **372**, 503–515.
37 M. Yang and M. Kurkinen, Chicken matrix metalloproteinase 22, *Handbook of Proteolytic Enzymes*, 2004.
38 D. Pei, T. Kang and H. Qi, *J. Biol. Chem.*, 2000, **275**, 33988–33997.
39 D. Moogk, I. P. da Silva, M. W. Ma, E. B. Friedman, E. V. de Miera, F. Darvishian, P. Scanlon, A. Perez-Garcia, A. C. Pavlick, N. Bhardwaj, P. J. Christos, I. Osman and M. Krogsgaard, *J. Transl. Med.*, 2014, **12**, 342.
40 E. Llano, A. M. Pendas, J. P. Freije, A. Nakano, V. Knauper, G. Murphy and C. Lopez-Otin, *Cancer Res.*, 1999, **59**, 2570–2576.
41 S. Kojima, Y. Itoh, S. Matsumoto, Y. Masuho and M. Seiki, *FEBS Lett.*, 2000, **480**, 142–146.
42 H. Yamamoto, A. Vinitketkumnuen, Y. Adachi, H. Taniguchi, T. Hirata, N. Miyamoto, K. Nosho, A. Imsumran, M. Fujita, M. Hosokawa, Y. Hinoda and K. Imai, *Carcinogenesis*, 2004, **25**, 2353–2360.
43 A. Cominelli, H. P. Gaide Chevronnay, P. Lemoine, P. J. Courtoy, E. Marbaix and P. Henriet, *Mol. Hum. Reprod.*, 2014, **20**, 767–775.
44 J. Lohi, C. L. Wilson, J. D. Roby and W. C. Parks, *J. Biol. Chem.*, 2001, **276**, 10134–10144.

45 T. T. Nguyen, D. Ding, W. R. Wolter, R. L. Perez, M. M. Champion, K. V. Mahasenan, D. Hesek, M. Lee, V. A. Schroeder, J. I. Jones, E. Lastochkin, M. K. Rose, C. E. Peterson, M. A. Suckow, S. Mobashery and M. Chang, *J. Med. Chem.*, 2018, **61**, 8825–8837.
46 N. Amara, M. Tholen and M. Bogyo, *ACS Chem. Biol.*, 2018, **13**, 2645–2654.
47 M. Morell, T. Nguyen Duc, A. L. Willis, S. Syed, J. Lee, E. Deu, Y. Deng, J. Xiao, B. E. Turk, J. R. Jessen, S. J. Weiss and M. Bogyo, *J. Am. Chem. Soc.*, 2013, **135**, 9139–9148.
48 A. Saghatelian, N. Jessani, A. Joseph, M. Humphrey and B. F. Cravatt, *Proc. Natl. Acad. Sci. U. S. A.*, 2004, **101**, 10000–10005.
49 S. A. Sieber, S. Niessen, H. S. Hoover and B. F. Cravatt, *Nat. Chem. Biol.*, 2006, **2**, 274–281.
50 J. R. Freije and R. Bischoff, *J. Chromatogr. A*, 2003, **1009**, 155–169.
51 D. Hesek, M. Toth, V. Krchnak, R. Fridman and S. Mobashery, *J. Org. Chem.*, 2006, **71**, 5848–5854.
52 D. Hesek, M. Toth, S. O. Meroueh, S. Brown, H. Zhao, W. Sakr, R. Fridman and S. Mobashery, *Chem. Biol.*, 2006, **13**, 379–386.
53 M. L. Moss and F. H. Rasmussen, *Anal. Biochem.*, 2007, **366**, 144–148.
54 Z. Peng, T. T. Nguyen, M. Wang, B. Anderson, M. M. Konai, V. A. Schroeder, W. R. Wolter, T. Page-Mayberry, C. E. Peterson, S. Mobashery and M. Chang, *ACS Chem. Biol.*, 2022, **17**, 1357–1363.
55 I. Botos, L. Scapozza, D. Zhang, L. A. Liotta and E. F. Meyer, *Proc. Natl. Acad. Sci. U. S. A.*, 1996, **93**, 2749–2754.
56 H. Laronha, I. Carpinteiro, J. Portugal, A. Azul, M. Polido, K. T. Petrova, M. Salema-Oom and J. Caldeira, *Biomolecules*, 2020, **10**, 717.
57 F. Grams, H. Brandstetter, S. D'Alo, D. Geppert, H. W. Krell, H. Leinert, V. Livi, E. Menta, A. Oliva, G. Zimmermann, F. Gram and V. E. Livi, *Biol. Chem.*, 2001, **382**, 1277–1285.
58 U. Schlomann, D. Wildeboer, A. Webster, O. Antropova, D. Zeuschner, C. G. Knight, A. J. Docherty, M. Lambert, L. Skelton, H. Jockusch and J. W. Bartsch, *J. Biol. Chem.*, 2002, **277**, 48210–48219.
59 T. Maretzky, S. Swendeman, E. Mogollon, G. Weskamp, U. Sahin, K. Reiss and C. P. Blobel, *Biochem. J.*, 2017, **474**, 1467–1479.
60 H. P. Hansen, B. Matthey, S. Barth, T. Kisseleva, T. Mokros, S. J. Davies, R. P. Beckett, R. Foelster-Holst, H. H. Lange, A. Engert and H. Lemke, *Int. J. Cancer*, 2002, **98**, 210–215.
61 J. I. Jones, T. T. Nguyen, Z. Peng and M. Chang, *Pharmaceuticals*, 2019, **12**, 79.
62 C. Masitas, Z. Peng, M. Wang, M. M. Konai, L. F. Avila-Cobian, L. Lemieux, J. Hovanesian, J. E. Grady, S. Mobashery and M. Chang, *ACS Pharmacol. Transl. Sci.*, 2022, **5**, 555–561.
63 Z. Peng, M. M. Konai, L. F. Avila-Cobian, M. Wang, S. Mobashery and M. Chang, *ACS Pharmacol. Transl. Sci.*, 2022, **5**, 555–561.
64 J. Y. Hsu, R. McKeon, S. Goussev, Z. Werb, J. U. Lee, A. Trivedi and L. J. Noble-Haeusslein, *J. Neurosci.*, 2006, **26**, 9841–9850.
65 A. Gutierrez-Fernandez, M. Inada, M. Balbin, A. Fueyo, A. S. Pitiot, A. Astudillo, K. Hirose, M. Hirata, S. D. Shapiro, A. Noel, Z. Werb, S. M. Krane, C. Lopez-Otin and X. S. Puente, *FASEB J.*, 2007, **21**, 2580–2591.
66 M. Muller, C. Trocme, B. Lardy, F. Morel, S. Halimi and P. Y. Benhamou, *Diabetic Med.*, 2008, **25**, 419–426.
67 Y. Liu, D. Min, T. Bolton, V. Nube, S. M. Twigg, D. K. Yue and S. V. McLennan, *Diabetes Care*, 2009, **32**, 117–119.
68 G. P. Ladwig, M. C. Robson, R. Liu, M. A. Kuhn, D. F. Muir and G. S. Schultz, *Wound Repair Regen.*, 2002, **10**, 26–37.
69 P. Liu, W. He and H. L. Chen, *J. Wound Ostomy Continence Nurse*, 2012, **39**, 495–499.
70 A. Pardo and M. Selman, *Proc. Am. Thorac. Soc.*, 2006, **3**, 383–388.
71 M. S. Espindola, D. M. Habiel, A. L. Coelho, B. Stripp, W. C. Parks, J. Oldham, F. J. Martinez, I. Noth, D. Lopez, A. Mikels-Vigdal, V. Smith and C. M. Hogaboam, *Am. J. Respir. Crit. Care Med.*, 2021, **203**, 458–470.
72 E. Ahrman, O. Hallgren, L. Malmstrom, U. Hedstrom, A. Malmstrom, L. Bjermer, X. H. Zhou, G. Westergren-Thorsson and J. Malmstrom, *J. Proteomics*, 2018, **189**, 23–33.
73 D. Lagares, P. Ghassemi-Kakroodi, C. Tremblay, A. Santos, C. K. Probst, A. Franklin, D. M. Santos, P. Grasberger, N. Ahluwalia, S. B. Montesi, B. S. Shea, K. E. Black, R. Knipe, M. Blati, M. Baron, B. Wu, H. Fahmi, R. Gandhi, A. Pardo, M. Selman, J. Wu, J. P. Pelletier, J. Martel-Pelletier, A. M. Tager and M. Kapoor, *Nat. Med.*, 2017, **23**, 1405–1415.
74 D. Q. Li, S. B. Lee, Z. Gunja-Smith, Y. Liu, A. Solomon, D. Meller and S. C. Tseng, *Arch. Ophthalmol.*, 2001, **119**, 71–80.
75 S. F. Yang, C. Y. Lin, P. Y. Yang, S. C. Chao, Y. Z. Ye and D. N. Hu, *Invest. Ophthalmol. Visual Sci.*, 2009, **50**, 4588–4596.
76 N. Di Girolamo, M. T. Coroneo and D. Wakefield, *Invest. Ophthalmol. Visual Sci.*, 2001, **42**, 1963–1968.
77 N. Dushku, M. K. John, G. S. Schultz and T. W. Reid, *Arch. Ophthalmol.*, 2001, **119**, 695–706.
78 I. Ulasov, R. Yi, D. Guo, P. Sarvaiya and C. Cobbs, *Biochim. Biophys. Acta*, 2014, **1846**, 113–120.
79 T. Abe, T. Mori, K. Kohno, M. Seiki, T. Hayakawa, H. G. Welgus, S. Hori and M. Kuwano, *Clin. Exp. Metastasis*, 1994, **12**, 296–304.
80 T. Itoh, M. Tanioka, H. Yoshida, T. Yoshioka, H. Nishimoto and S. Itohara, *Cancer Res.*, 1998, **58**, 1048–1051.
81 V. Thakur, V. S. Thakur, B. Aguila, T. I. Slepak, M. Wang, W. Song, M. Konai, S. Mobashery, M. Chang, A. B. Rana, D. Wang, J. T. de Freitas, S. Humayun Gultekin, S. M. Welford, M. E. Ivan and B. Bedogni, *Neurooncol Adv.*, 2022, **4**, vdac147.
82 G. B. Fields, *Cells*, 2019, **8**, 984.
83 S. Mondal, N. Adhikari, S. Banerjee, S. A. Amin and T. Jha, *Eur. J. Med. Chem.*, 2020, **194**, 112260.
84 A. Winer, S. Adams and P. Mignatti, *Mol. Cancer Ther.*, 2018, **17**, 1147–1155.

85 V. Arkadash, G. Yosef, J. Shirian, I. Cohen, Y. Horev, M. Grossman, I. Sagi, E. S. Radisky, J. M. Shifman and N. Papo, *J. Biol. Chem.*, 2017, **292**, 3481–3495.
86 Q. Yao, L. Kou, Y. Tu and L. Zhu, *Trends Pharmacol. Sci.*, 2018, **39**, 766–781.
87 R. E. Vandenbroucke and C. Libert, *Nat. Rev. Drug Discovery*, 2014, **13**, 904–927.
88 T. W. Chung, S. K. Moon, Y. C. Chang, J. H. Ko, Y. C. Lee, G. Cho, S. H. Kim, J. G. Kim and C. H. Kim, *FASEB J.*, 2004, **18**, 1670–1681.
89 Y. Yordanov, *Pharmacia*, 2019, **66**, 107–114.
90 M. A. Shah, A. Starodub, S. Sharma, J. Berlin, M. Patel, Z. A. Wainberg, J. Chaves, M. Gordon, K. Windsor, C. B. Brachmann, X. Huang, G. Vosganian, J. D. Maltzman, V. Smith, J. A. Silverman, H. J. Lenz and J. C. Bendell, *Clin. Cancer Res.*, 2018, **24**, 3829–3837.
91 M. A. Shah, G. Bodoky, A. Starodub, D. Cunningham, D. Yip, Z. A. Wainberg, J. Bendell, D. Thai, J. He, P. Bhargava and J. A. Ajani, *J. Clin. Oncol.*, 2021, **39**, 990–1000.
92 Z. Peng, T. T. Nguyen, W. Song, B. Anderson, W. R. Wolter, V. A. Schroeder, D. Hesek, M. Lee, S. Mobashery and M. Chang, *ACS Pharmacol. Transl. Sci.*, 2021, **4**, 107–117.
93 B. Lan, L. Zhang, L. Yang, J. Wu, N. Li, C. Pan, X. Wang, L. Zeng, L. Yan, C. Yang and M. Ren, *J. Nanobiotechnol.*, 2021, **19**, 130.